

A Study on Sinus-lifting Motion of a Snake Robot with Sequential Optimization of a Hybrid System

Satoshi Toyoshima, Motoyasu Tanaka, *Member, IEEE*, and Fumitoshi Matsuno, *Member, IEEE*,

Abstract—In this paper, we consider “sinus-lifting motion” of a living snake, in which a snake lifts up some parts of its body from the ground, and switches the lifted parts dynamically. It is not clear whether imitating the sinus-lifting motion is the best locomotion or not for a snake like robot. The aim of this paper is to propose an appropriate motion pattern to a snake like robot considering the optimality of the sinus-lifting motion. We introduce two physical parameters, constraint forces and energy efficiency, as cost functions to optimize and propose switching strategies for generating optimal motion patterns of a snake like robot.

Note to Practitioners —The biologically inspired robots have been researched and developed intensely. Many researchers expect that the locomotion of living things has high locomotion performance in natural world, because they have survived by natural selection. However, when we consider the effectiveness of imitating the biological locomotion, it is important that we clarify not only the kinematical and dynamical features of the locomotion but also the principle of the locomotion, which means the reason why a living thing achieved the locomotion. We expect that the knowledge regarding the principle of the locomotion suggests a more effective motion pattern which is specific to mechanical robots. In this study, we focus on the creeping locomotion of a living snake. Practically the great ability of movement of a living snake is useful, for example search and rescue missions at disaster sites, so snake-like robots have been developed. Based on the hybrid model we discuss the optimal locomotion of the snake robot with comparing locomotion of a living snake.

Index Terms—Biologically inspired robots, Snake robots, Hybrid systems, Optimality, Serpenoid curve

I. INTRODUCTION

ALIVING SNAKE has simple body shape without arms and legs, but it has great ability of movement, for example, climbing a tree, swimming, and so on. Since this ability is useful for inspection of pipelines and inside of debris at disaster sites due to its slim body shape, snake like robots have been developed [1]–[6]. The unique locomotive capabilities of snakes have been researched in order to understand the potential of them and to realize them by artifacts. As pointed out by Hirose [1], the first experimental and quantitative research of snake locomotion was done by Gray [7]. Gray analyzed the mechanics of several types of the snake locomotion from biological point of view. Hirose studied the biomechanics of snakes and modeled a real snake by a wheeled multi-link mechanism (Passive wheels are attached to the sides of the snake robot body.) based on the observations [1]. “Sinus-



Fig. 1. Sinus-lifting motion of a snake [8]

lifting motion” (Fig. 1) is one of a unique locomotion of a living snake. This motion is used for rapid movement and a snake lifts up the section of the body around the position with maximum curvature of the body shape from the ground [1]. Hirose described it as an effective type of locomotion such that the snake centers its weight on the part of its body that can easily slide on, so that the slippage possibility between body and environment decreases. Shigeta et al. [9] and Tsuda et al. [10] considered the relationship between proposed dynamic manipulability and sinus-lifting motion. Ma et al. derived a model of a 3-dimensional snake robot without passive wheels considering Coulomb friction for the interaction with the environment and compared the simulation results of the normal serpentine locomotion and the sinus-lifting locomotion from the point of view of dynamics [11]. Yamada and Hirose proposed a control method of a snake like robot, which has extremely large number of degree of freedom, based on a continuous curve approximation and analyzed the effectiveness of the sinus-lifting motion by simulation and experiments [12]. However, in these previous studies the grounded parts of the body are determined by a heuristic way: “The body around the position of maximum curvature should be lifted up.” It is hard to clarify how to decide the grounded parts from among its whole body and the reason why a living snake achieves this motion from these results. Therefore the purposes of our research are to analyze the sinus-lifting motion in terms of optimization of the motion pattern and to propose the most effective motion pattern for a snake like robot. Moreover analysis on the optimality of another locomotions of a living snake will be discussed as a long-term goal.

In this paper we discuss a snake robot based on the wheeled multi-link mechanism (a wheeled snake robot). We adopt two physical parameter as a cost function. The first parameter is a constraint force of a passive wheel. The reason why we adopt the constraint forces as a cost function is that it has been referred in previous researches [1] [11] [12]. They pointed out that the motion pattern of the sinus-lifting is effective for the prevention of sliding of the snake robot body out of its track (sideslip). The wheeled snake robot will be able to reduce

Manuscript received ; revised .

S. Toyoshima and F. Matsuno are with Kyoto University, Kyotodaigaku-Katsura, Nishikyo-ku, Kyoto, Japan (e-mail: matsuno@me.kyoto-u.ac.jp).

M. Tanaka is with The University of Electro-Communications (e-mail: mtanaka@uec.ac.jp).

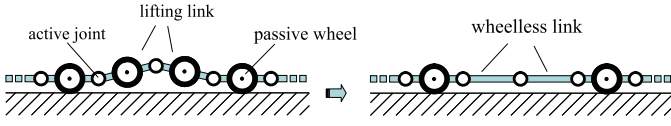


Fig. 2. Modeling of lifting links as wheel-less links

possibility of the sideslip and generate an effective locomotion by minimizing constraint forces. The second parameter is energy efficiency. It is considered that quadrupeds, such as a horse and a dog, change their gait as to minimize their energy consumption [13], and it seems reasonable that snakes also choose the motion pattern based on the energy efficiency.

We consider the wheeled snake robot model which can arbitrarily change states of wheels as lifting up or grounding state. This switching mechanism of the states is modeled by a hybrid system. Based on this hybrid model we propose control strategies for switching motion pattern of the robot that optimizes each criterion. And then, by simulation, we compare the generated motion patterns with the sinus-lifting motion of a living snake and discuss the relationship between the two parameters and the optimal motion pattern of the wheeled snake robot.

II. MODEL

We consider an n link wheeled snake robot. All wheels are passive and all joints are active, and we assume that a passive wheel does not slide sideways and that the environment is flat. The lifting links of the snake robot are regarded as the wheel-less links of the 2D snake robot, and the grounded links are regarded as the wheeled links as shown Fig. 2. In other words, the lifting up motion of the snake in 3D space is modeled by switching the wheeled link to the wheel-less link in the 2D motion. We assume that the time taken for lifting up and grounding the wheels is negligible. We call the state of allocation of wheeled links and wheel-less links as “modes” and set the number of modes as N .

We use the model of the snake robot, which is proposed in [14][15][16]. Let $\mathbf{r} = [x_h, y_h]^T$ be the position of the snake head, θ_h be the attitude of the snake head, $\phi = [\phi_1, \dots, \phi_{n-1}]^T$ be the relative joint angles of each link, $\boldsymbol{\tau} = [\tau_1, \dots, \tau_{n-1}]^T$ be the joint torques, $\boldsymbol{\theta} = [\theta_h, \phi_1, \dots, \phi_{n-1}]^T = [\theta_1, \dots, \theta_n]^T$ be the joint variables.

We consider the n -link wheeled snake robot of the σ -th mode, where $\sigma \in M$, $M = \{1, 2, \dots, N\}$. In the σ -th mode the passive wheels of the m_σ -th link ($m_\sigma \in \Lambda_\sigma$, where Λ_σ is an index set related to the lifted links) are removed and let us set the number of the wheel-less links of the σ -th mode as n_σ . Let ΔT be the switching time period and $t_k = k\Delta T$ ($k = 0, 1, 2, \dots$) be the switching time. The system of the snake robot is expressed as a following hybrid system

$$\begin{aligned} \tilde{M}_{\sigma(t)} \ddot{\mathbf{w}}_{\sigma(t)} + (\tilde{C}_{\sigma(t)} + \tilde{D}_{\sigma(t)}) \dot{\mathbf{w}}_{\sigma(t)} &= \tilde{E}_{\sigma(t)} \boldsymbol{\tau} \\ \sigma(t) &= \sigma(t_k), \quad \forall t \in [t_k, t_{k+1}) \end{aligned} \quad (1)$$

where $\tilde{\mathbf{w}}_\sigma = [\mathbf{r}^T \tilde{\phi}_\sigma^T]^T$ is the set of state variables corresponding to the mode σ , and $\tilde{\phi}_\sigma = [\theta_{j_1}, \dots, \theta_{j_{n_\sigma}}]^T$ is the set of the shape controllable points corresponding to the wheel-less links, which are variables representing kinematic redundancy [14]. We assume that $(n - n_\sigma) \geq 3$ is satisfied to make the

system redundancy controllable [14][17]. Thus, the minimum number of grounded links is three [17].

In this dynamic equation (1), \tilde{M}_σ is a reduced order inertia matrix, \tilde{C}_σ is a reduced order matrix regarding Coriolis' and centrifugal forces, \tilde{D}_σ is a reduced order friction matrix. In this study, we introduce the three types of the viscous friction which causes energy loss in the creeping locomotion. The first one is translational friction between a link and the ground and its coefficient is set as d_{xy} . The second one is rotational friction between a link and the ground and its coefficient is set as d_θ . The third one is rotational friction of a joint and its coefficient is set as d_ϕ . The matrix \tilde{D}_σ is composed of the friction coefficients d_{xy} , d_θ , and d_ϕ . That is to say, in this hybrid system model the viscous frictions regarding d_{xy} and d_θ do not cause energy loss, if the wheels are lifted up.

III. BODY CURVE AND CONTROL INPUT

One of the aim of this study is to analyze the sinus-lifting locomotion of a living snake based on a dynamic model of a snake robot. We employ serpenoid curve [1] for the body shape of the robot. Serpenoid curve is defined as the curve whose curvature varies in sinusoidal manner with respect to the arc-length coordinate. This curve is said to be very similar to the body shape of biological snakes.

To employ the body shape, we set the yaw joint angles as

$$\phi_p(t) = \frac{2\pi T}{n} \alpha \sin \left(vt - \frac{2\pi T}{n} p \right), \quad p = 1, \dots, n-1, \quad (2)$$

where v is the velocity of bending and T indicates how many periods are formed within the body. The winding angle α is defined as a maximum angle between the body shape and the direction of movement. For the snake robot of the σ -th mode, $\dot{\mathbf{w}}_\sigma$ and $\ddot{\mathbf{w}}_\sigma$ can be obtained using the kinematic model [15], and the input torque $\boldsymbol{\tau}_\sigma$ is also obtained by calculating the forward dynamics of (1). In the case in which the number of inputs ($n-1$) is larger than the number of state variables ($2+n_\sigma$), i.e., $(n-n_\sigma) > 3$ for any σ -th mode, the number of rows of $\tilde{E}_\sigma \in \mathbf{R}^{(2+n_\sigma) \times (n-1)}$ is larger than that of columns of \tilde{E}_σ and the input is expressed as

$$\boldsymbol{\tau}_\sigma = \tilde{E}_\sigma^\dagger \left(\tilde{M}_\sigma \ddot{\mathbf{w}}_\sigma + (\tilde{C}_\sigma + \tilde{D}_\sigma) \dot{\mathbf{w}}_\sigma \right) + \boldsymbol{\tau}_{ker} \quad (3)$$

where $\tilde{E}_\sigma^\dagger = \tilde{E}_\sigma^T (\tilde{E}_\sigma \tilde{E}_\sigma^T)^{-1}$, $\boldsymbol{\tau}_{ker} \in \text{Ker}(\tilde{E}_\sigma)$ is an arbitrary vector in $\text{Ker}(\tilde{E}_\sigma)$.

We determine $\boldsymbol{\tau}_{ker}$ according to the evaluation criteria. In the case of minimizing the constraint forces we employ $\boldsymbol{\tau}_{ker}$ which minimizes the l_2 -norm of the constraint force $\|\mathbf{f}_\sigma\|$ proposed in [15], where \mathbf{f}_σ is the constraint forces of the σ -th mode. In the case of minimizing the energy consumption we employ $\boldsymbol{\tau}_{ker} = 0$ which minimizes the l_2 -norm of the input torque $\|\boldsymbol{\tau}_\sigma\|$ of the creeping motion.

We have another freedom of the mode switching. In the next section we introduce evaluation criteria to select an optimal mode.

IV. EVALUATION CRITERIA FOR MODE SELECTION

In this section, we define the constraint force and the consumed energy, and introduce the evaluation criteria.

A. Evaluation criterion based on constraint force

1) *Constraint forces*: We assume that the j -th link of the snake robot of the σ -th mode is wheeled. Let us define $f_{\sigma j}$ as the constraint force of the j -th link of the σ -th mode and $\mathbf{f}_{\sigma} \in \mathbf{R}^{(n-n_{\sigma})}$ as a vector of all constraint forces of the σ -th mode. Then, \mathbf{f}_{σ} is expressed as follows [14]

$$\mathbf{f}_{\sigma} = X_{\sigma}\boldsymbol{\tau} + Y_{\sigma} \quad (4)$$

where X_{σ} is the transformation matrix from the torque to the constraint force and Y_{σ} is the nonlinear term related to the velocity.

2) *Evaluation criterion*: If the motion pattern of the sinus-lifting is designed to prevent the slipping in the normal direction of the body [1], the constraint force in the sinus-lifting motion would become smaller than that in the normal creeping locomotion. Therefore, we evaluate the slipping with the l_2 -norm of the constraint force $\|\mathbf{f}_{\sigma}\| = \sqrt{\mathbf{f}_{\sigma}^T \mathbf{f}_{\sigma}}$ and minimize it in order to realize the motion to reduce danger of the sideslipping.

B. Evaluation criterion based on energy consumption

In this paper, we consider utilizing a geared DC motor as a joint actuator which is required to generate the locomotion of the snake robot. Let us define the consumed energy of DC motors as follows [18]

$$e = \int \delta(\boldsymbol{\tau}^T(t)\boldsymbol{\omega}(t)) + \gamma\|\boldsymbol{\tau}(t)\|^2 dt \quad (5)$$

where

$$\delta(x) = \begin{cases} 0 & x \leq 0 \\ x & x > 0 \end{cases}, \quad (6)$$

and $\boldsymbol{\tau}$ is a torque vector, $\boldsymbol{\omega}$ is an angular velocity vector of the motors, and $\gamma = R/k^2$ (R is resistance and k is a torque coefficient of the motor). In (5), the first term means the mechanical work and the second term means the heat energy loss due to the Joule heat. We assume that the lifting motion has no dynamical influence on the 2D creeping motion given by (1).

The energy consumption is caused by the yaw motion for creeping and pitch motion for the mode switching. Moreover, the energy consumption of the pitch motion is divided into following two parts, *i.e.* the energy consumed for lifting up/grounding the body and the energy consumed for holding lifted up parts of the body. In this paper, these categories of energy consumption are called the “creeping energy”, the “lifting energy”, and the “holding energy”, respectively. In our previous research [16] these energy models are described in detail.

1) *Creeping energy*: In the creeping motion, the angular velocity $\boldsymbol{\omega}$ is given by (2) and the torque $\boldsymbol{\tau}$ is given by (3), where we employ $\boldsymbol{\tau}_{ker} = 0$ in order to minimize this creeping energy consumption. Therefore, the creeping energy for the σ_k -th mode consumed from $t = t_k$ during the switching time period ΔT is defined as follows

$$E_{creep, \sigma_k} = \int_{t_k}^{t_{k+1}} \delta(\bar{\boldsymbol{\tau}}_{\sigma_k}^T(t)\dot{\boldsymbol{\phi}}(t)) + \gamma_{creep}\|\bar{\boldsymbol{\tau}}_{\sigma_k}(t)\|^2 dt \quad (7)$$

where $t_{k+1} = t_k + \Delta T$,

$$\dot{\boldsymbol{\phi}} = r_{creep}\dot{\boldsymbol{\phi}}, \quad \bar{\boldsymbol{\tau}}_{\sigma_k} = \frac{1}{r_{creep}}\boldsymbol{\tau}_{\sigma_k}, \quad (8)$$

r_{creep} and γ_{creep} are the gear reduction ratio of the DC motors utilized for the creeping motion and the coefficient corresponding to γ in (5) of the DC motors utilized for the holding motion, respectively.

2) *Lifting energy*: On the assumption that the time taken for shifting the mode and its dynamics are negligible, the lifting energy at t_k is defined by the absolute amount of changes of potential energy of all links as follow [16].

$$E_{lift, \sigma_k} = \sum_{i=1}^{n-1} E_{i, \sigma_{k-1} \sigma_k} \quad (9)$$

where $E_{i, \sigma_{k-1} \sigma_k}$ is the amount of potential energy change of the i -th link for the switching from the σ_{k-1} -th mode for $[t_{k-1}, t_k)$ to the σ_k -th mode at t_k .

3) *Holding energy*: From (5), the holding energy in the case of the σ_k -th mode for $[t_k, t_{k+1})$ is given by

$$E_{hold, \sigma_k} = \int_{t_k}^{t_{k+1}} \gamma_{hold}\|\hat{\boldsymbol{\tau}}'_{\sigma_k}(t)\|^2 dt \quad (10)$$

where

$$\hat{\boldsymbol{\tau}}'_{\sigma_k} = \frac{1}{r_{hold}}\hat{\boldsymbol{\tau}}_{\sigma_k} \quad (11)$$

where $\hat{\boldsymbol{\tau}}_{\sigma_k}$ is the joint torque required to hold up the body, r_{hold} and γ_{hold} are the gear ratio and the coefficient corresponding to γ in (5) of the DC motor utilized for the holding motion, respectively.

4) *Evaluation criterion*: When the snake robot switches its mode from the σ_{k-1} -th mode for $[t_{k-1}, t_k)$ to the σ_k -th mode at t_k , let us define the total energy E_{total, σ_k} consumed from current time t_k during the switching time period ΔT as an evaluation criterion by

$$E_{total, \sigma_k} = E_{creep, \sigma_k} + E_{lift, \sigma_k} + E_{hold, \sigma_k}. \quad (12)$$

In the next section we consider the switching strategies to minimize the constraint force and to minimize the total energy consumption.

V. SWITCHING OF MODES

A. Optimization problems

To optimize the switching motion we introduce two evaluation functions: the constraint forces and the energy efficiency for the time period $[t_k, t_{k+1})$.

Additionally, we consider the switching conditions for stable locomotion of the snake robot when its mode is changed. We assume that the mode is σ_k at $t = t_k$. Let $C_G(t_k)$ be the center of gravity of the whole body of the snake robot, and $P(\mathbf{q}(t_k); \sigma_k)$ be the supporting polygon constructed by the passive wheels of the grounded links. We introduce the following condition

$$C_G(t) \in P(\mathbf{q}(t); \sigma_k), \quad t_k \leq t < t_{k+1}. \quad (13)$$

Condition (13) means that the snake robot is static stable during $t_k \leq t < t_{k+1}$. The snake robot satisfies the static stability of the gait by introducing this condition. By considering the above condition, we design the selection strategy of the mode σ in (1).

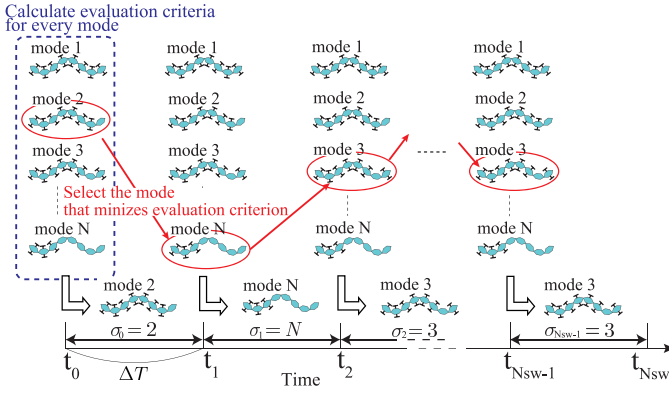


Fig. 3. Mode selection based on the minimization of evaluation criterion

When we select the motion pattern that minimizes the constraint force, we adopt the following equation (14) as the corresponding evaluation function.

$$\min_{\sigma} \left\{ \max_{t_k \leq t < t_{k+1}} \|f_{\sigma}(t)\| \right\} \quad (14)$$

subject to eq.(13)

On the other hand, when we select the motion pattern that minimizes the energy consumption, we adopt the following equation (15) as the corresponding evaluation function.

$$\min_{\sigma} \{E_{total, \sigma(t)} / \Delta x_k\}, \quad t_k \leq t < t_{k+1} \quad (15)$$

subject to eq.(13)

where Δx_k is the moving distance during $[t_k, t_{k+1})$.

We can obtain the optimal mode σ that minimizes each evaluation criterion by solving the optimization problem (14) or (15). In this study, we fix the number of times of the mode switching N_{sw} , which means that the snake robot switches its mode N_{sw} times per one cycle of the creeping motion regardless of the locomotion velocity.

B. Optimal motion pattern

Before we discuss the simulation, we summarize the way to generate an optimal motion pattern in our simulation. In this study, the locomotion of the snake robot is given based on the serpenoid curve as described by (2), in other words, the states variables (joint angles ϕ , joint velocities $\dot{\phi}$, and joint accelerations $\ddot{\phi}$) are given. And then we can obtain the input torque τ for a given mode which generates the intended locomotion by calculating the forward dynamics (3). The constraint force (4) or the energy efficiency (12) for the given mode can be calculated by using the obtained input torque. Finally, we can select the grounded pattern that optimizes the evaluation criterion expressed by (14) for the constraint force or by (15) for the energy efficiency from all admissible modes at each switching time t_k . We use a full search for solving the optimization problems (14) and (15). As shown in Fig. 3, we calculate the evaluation criteria of the next period at $t = t_k$ for every modes and select the next mode that minimizes it. We consider this generated motion as the optimal motion pattern of the wheeled snake like robot.

Body shape			
T=1.5	$\alpha = 0.1$	$\alpha = 0.5$	$\alpha = 0.9$

Fig. 4. Body shapes for $T = 1.5$ and $\alpha = 0.1, 0.5, 0.9$

TABLE I
VELOCITY OF THE SNAKE ROBOT ALONG THE DIRECTION OF MOVEMENT
FOR VARIOUS PARAMETER SETS OF α AND n_v

α [rad]	n_v			
	1	5	9	13
0.2	0.031m/s	0.15m/s	0.27m/s	0.40m/s
0.6	0.028m/s	0.14m/s	0.25m/s	0.36m/s
1.0	0.021m/s	0.12m/s	0.19m/s	0.30m/s

VI. SIMULATION RESULTS AND DISCUSSION

In this section, we analyze the relationship between the switching of modes based on each evaluation criterion and the generation of the sinus-lifting motion by simulation. We consider an 8-link snake robot where the length of each link is 0.05[m], mass of each link is 0.5[kg], and moment of inertia of each link is 1.0×10^{-3} [kgm²]. In this case, the number of modes is $N = 219$.

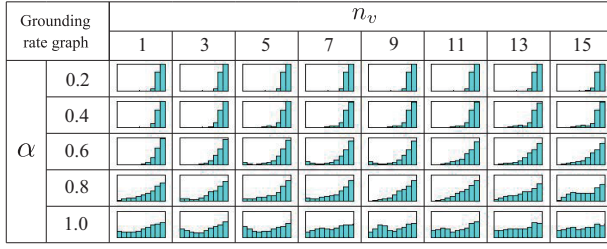
We set $t_0 = 0$, $t_{Nsw} = 15$, and the parameters of the body curve (2) are set as $v = (2\pi/15)n_v$ [rad/s], $n_v = 1, 3, \dots, 15$, where n_v is an index of the velocity and means the number of cycle which the snake robot moves during simulation time, $T = 1.5$, $\alpha = 0.1, 0.2, \dots, 1.0$ [rad], and $N_{sw} = 25$. Table I shows velocity of the snake robot along the direction of movement for various parameter sets of α and n_v . The frictional coefficients described in Sec. II are set as $d_{xy} = 1.0$ [Ns/m], $d_{\theta} = 0.05$ [Nsm], and $d_{\phi} = 0.1$ [Nsm]. In (7) and (10), the motor and gear mechanism are selected from “maxon motor 2010/11” and the values are set as $\gamma_{creep} = 4.6 \times 10^4$ [Ω(A/Nm)²], $\gamma_{hold} = 8.1 \times 10^2$ [Ω(A/Nm)²] and the gear reduction ratios are $r_{creep} = 76$ and $r_{hold} = 51$. The maximum velocity of this snake robot is $n_v = 15$, which is decided by the intermittently permissible torque of the motor and gear mechanism. The body curves for $\alpha = 0.1, 0.5, 0.9$ in the case of $T = 1.5$ are shown in Figure 4.

In this study, we introduce the “grounding rate graph”, which is derived in [15], as an evaluation index of the sinus-lifting motion. This graph shows the grounding rate of each part of the body. The horizontal axis shows the absolute value Ψ of the angle between the body curve and the direction of locomotion and is divided several regions. The vertical axis shows the grounding time rate during the snake robot goes through each region of Ψ . It is considered that, in the case of sinus-lifting motion, the left side of the graph is low grounding rate and the right side of it is high grounding rate. In our previous research [16] the definition and mathematical formulation of this graph is described in detail.

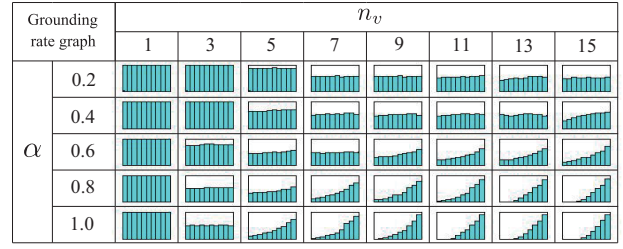
A. Optimal motion pattern based on each evaluation criteria

Figure 5 shows the grounding rate graphs for various parameter sets of α and n_v . Fig. 5(a) is given by the switching strategy to minimize the constraint force and Fig. 5(b) is given by that to minimize the total energy consumption.

From Fig. 5(a), we find that the sinus-lifting motion is generated in many sets of parameters. It is well known that



(a) Evaluation criteria: the constraint forces

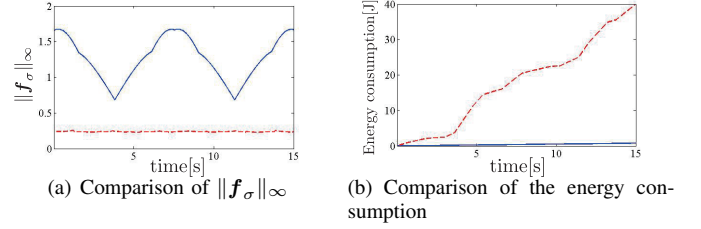


(b) Evaluation criteria: the energy efficiency

Fig. 5. Grounding rate graphs for various parameter sets of α and n_v

a living snake grounds all parts of the body in the case of slow movement and changes the motion pattern depending on its locomotion speed. However, from Fig. 5(a) we cannot explain the phenomena. This result indicates that the snake robot should not adopt the motion pattern like a living snake and the norm of the constraint force is not a good evaluation function for understanding the snake locomotion. On the other hand, in the case of minimization of the energy consumption, we can find these phenomena. As indicated in Fig. 5(b), from grounding rate graphs of the first column we find that the mode which all links are grounded is the most efficient motion pattern for the slow movement ($n_v = 1$) regardless of changing the winding angle α . From grounding rate graphs of each row corresponding to $\alpha = 0.6, 0.8, 1.0$ of Fig. 5(b) we find that the most efficient motion pattern for the rapid movement (big value of n_v , e. g., $n_v = 15$) attains a closer motion to the sinus-lifting. We calculate the constraint force and the energy consumption in the case $\alpha = 0.2, 0.4, 0.6, 0.8, 1.0$, $n_v = 1$ for the slow movement. Figure 6 shows the comparison of the infinity norm of the constraint force and the energy consumption in the representative case of $(\alpha, n_v) = (0.2, 1)$. In Fig. 6, the red broken line shows the value for the minimization of the constraint force (corresponding to Fig. 5(a)) and the blue solid line shows the value for the optimization of the energy efficiency (corresponding to Fig. 5(b)). From Fig. 6(a) we find that the maximum values of the constraint force for each evaluation function are not big difference. We can find that the sinus-lifting motion generated by the minimization of the constraint force is inefficient about 20 times of the normal creeping locomotion generated by the optimization of the energy efficient from Fig. 6(b). This results indicate that, if there is sufficient friction between the robot and environment, the snake robot should adopt the normal creeping locomotion pattern based on the optimization of the energy efficiency. The qualitative nature of the conclusion is not different regardless of the change of α .

Next, we analyze the optimal motion pattern at high speed locomotion. From Fig. 5 we can find that the sinus-lifting motion is the optimal motion pattern for the rapid movement (e. g., $n_v = 13, 15$) corresponding to appropriate values of α . As shown in Fig. 5(a), the optimal motion patterns based on minimizing the constraint forces is different from the sinus-lifting motion for large α (e. g., $\alpha = 0.8, 1.0$, $n_v = 13, 15$). On the other hand, Fig. 5(b) shows that the larger the value α , the closer to the sinus-lifting the motion becomes. Figure 7 shows comparison of the maximum value of

Fig. 6. Comparison of value of the constraint force and the energy consumption for the minimization of the constraint force (- -) and the optimization of the energy efficiency (—) in the case of $(\alpha, n_v) = (0.2, 1)$.

the constraint force $\max_{t_0 \leq t \leq t_{N_{sw}}} \|f_{\sigma}(t)\|_{\infty}$ (red broken lines) for one cycle movement $[t_0, t_{N_{sw}}]$ and the energy efficiency $\sum_{k=1}^{N_{sw}} E_{total, \sigma_k} / \Delta x_k$ (blue solid lines) corresponding to each evaluation criterion for the fast movement $n_v = 15$ and $\alpha = 0.2, 0.4, \dots, 1.0$. Figure 7(a) and (b) show the comparisons corresponding to the minimization of the constraint force and the optimization of the energy efficiency, respectively. From Fig. 7(a)(b) we can find that the larger the value α , the smaller the constraint force becomes, and the smaller the value α , the better the energy efficiency becomes, regardless of the evaluation criteria. We can find same qualitative property obtained from Fig. 7 ($n_v = 15$) for $n_v = 11, 13$. From Figs. 5(a) and 7(a) we find that, when the body shape of the snake robot makes it easy to slide (the large constraint force is generated) corresponding to the small α (0.2 and 0.4), the sinus-lifting motion is the best motion pattern for the prevention of the sideslip for the fast movement. Moreover, from Figs. 5(b) and 7(b) we find that, when the energy efficiency is not good due to the large α (0.8 and 1.0), the sinus-lifting is also the best motion pattern of reducing the energy consumption for the fast movement. The prevention of the sideslip and the reduction of the energy consumption are both important for efficient locomotion of the snake robot. For this reason, in the next subsection, we propose a combinational optimization problem and analyze the optimal motion pattern which takes both evaluation criteria into account at the same time.

B. Combinational optimization problem

We propose a new optimization problem as follow

$$\min_{\sigma} \{a(\max_t \|f_{\sigma}(t)\|) + bE_{total, \sigma(t)} / \Delta x_k\} \quad (16)$$

$$, t_k \leq t < t_{k+1}$$

where a and b are weight coefficients which are introduced in order to adjust the scale difference of the constraint force

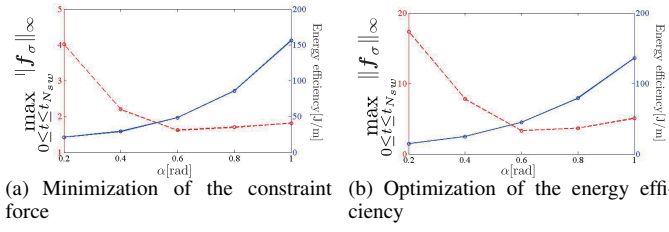


Fig. 7. Comparison of value of the constraint force (---) and the energy efficiency (—) at the rapid movement ($n_v = 15$).

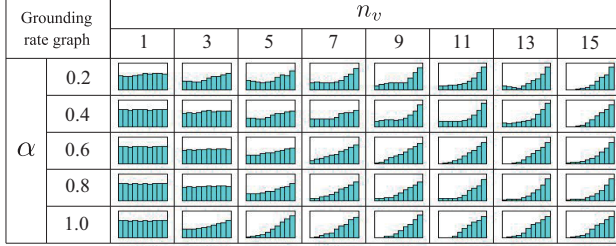


Fig. 8. Grounding rate graphs for a combinational evaluation criterion

and the energy efficiency. Figure 8 shows the grounding rate graphs of the optimal motion patterns generated by (16) in the case of $(a, b) = (5, 1)$. The results of Fig. 8 indicate that the sinus-lifting motion is the best motion pattern for the rapid movement ($n_v = 13, 15$) regardless of the body shape α . Figure 9 shows the maximum value of the constraint force (red broken line) and the energy efficiency (blue solid line) of one cycle same as Fig. 7 for $n_v = 15$ and $\alpha = 0.2, 0.4, \dots, 1.0$. From this figure, we can observe the sinus-lifting motion generated by this combinational optimization can solve a trade-off of the reduction between the constraint force and the energy consumption. On the other words, these results suggest that there is a benefit of imitating the sinus-lifting motion for the rapid movement of the wheeled snake like robot in terms of the energy efficiency and the prevention of the sideslip.

VII. CONCLUSION

In this paper, we considered the switching of grounded points of the wheeled snake robot and obtained the optimal motion patterns. The results of our simulation show that, the switching strategy based on the minimization of the constraint force cannot describe the change of the optimal motion pattern corresponding to the locomotion speed that a living snake has. On the other hand, in the case of the minimization of the energy efficiency, the simulation result is in good agreement with the phenomena observed by a living snake. Moreover, we find that the sinus-lifting motion is the optimal motion pattern for the rapid movement, when we consider both evaluation criteria at the same time.

On the point of view of robotics, the results show that there is a benefit of imitating the sinus-lifting motion for the snake robot in terms of realization of effective locomotion. The fact that, when the snake robot moves rapidly, the sinus-lifting motion is the best locomotion pattern for suppressing the constraint force and the energy consumption at the same time. We can predict that a real snake switches grounded parts of its body based on a trade-off between the reduction of the constraint force and the energy efficiency. We should consider

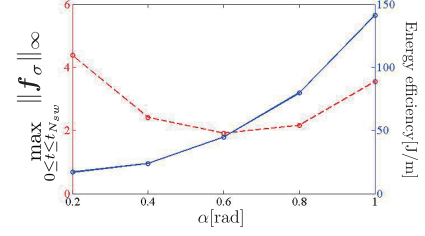


Fig. 9. The maximum value of the constraint force and the energy efficiency in the case of a combinational evaluation criterion

an energy model of musculoskeletal system to confirm our conclusion for a living snake. It is one of our future problems. Additionally, we will demonstrate the simulation result by an experiment with a wheeled snake robot.

REFERENCES

- [1] S. Hirose, *Biologically Inspired Robots (Snake-like Locomotor and Manipulator)*, Oxford University Press, 1993.
- [2] G. S. Chirikjian and J. W. Burdick, "The Kinematics of Hyper-Redundant Robot Locomotion," *IEEE Trans. on Robotics and Automation*, Vol. 11, pp.781–793, 1995.
- [3] J. W. Burdick, J. Radford, and G. S. Chirikjian, "A "Sidewinding" Locomotion Gait for Hyper-Redundant Robots", *Proc. IEEE Int. Conf. on Robotics and Automation*, Vol. 3, pp. 101-106, 1993.
- [4] C. Wright, A. Johnson, A. Peck, Z. McCord, A. Naaktgeboren, P. Gianfortoni, M. Gonzalez-Rivero, R. Hatton and H. Choset, "Design of a Modular Snake Robot," *Proc. IEEE/RSJ Int. Conf. on Intelligent Robots and Systems*, pp.2609-2614, 2007.
- [5] K. Lipkin, I. Brown, A. Peck, H. Choset, J. Rembisz, P. Gianfortoni, and A. Naaktgeboren, "Differentiable and Piecewise Differentiable Gaits for Snake Robots," *Proc. IEEE/RSJ Int. Conf. on Intelligent Robots and Systems*, pp.1864-1869, 2007.
- [6] P. Liljebäck, K. Pettersen, Ø. Stavdahl, and J. Grasdahl, "Controllability and Stability Analysis of Planar Snake Robot Locomotion", *IEEE Trans. on Automatic Control*, Vol. 56, No. 6, 2011
- [7] J. Gray, "The Mechanism of locomotion in Snakes," *J. of Experimental Biology*, Vol. 23, No. 2, pp. 101-123, 1946.
- [8] <http://www.youtube.com/watch?v=zEto1-ZTbd4&list=PL2F7D624D8E886E68&index=11>
- [9] K. Shigeta, H. Date, S. Nakaura and M. Sampei, "Improvement of Manipulability for Locomotion of a Snake Robot by Mass Distribution," *Proc. SICE Annual Conference 2002*, pp. 2214-2217, 2002.
- [10] M. Tsuda, S. Nakaura and M. Sampei, "Dynamic Manipulability of a Snake-like Robot and its Effect for Sinus-lifting Motion," *Proc. SICE Annual Conference 2004*, pp. 2202-2207, 2004.
- [11] S. Ma, Y. Ohmameuda and K. Inoue, "Dynamic Analysis of 3-dimensional Snake Robots," *Proc. IEEE/RSJ Int. Conf. on Intelligent Robots and Systems*, pp.767-772, 2004.
- [12] H. Yamada and S. Hirose, "Study of Active Cord Mechanism—Generalized Basic Equations of the Locomotive Dynamics of the ACM and Analysis of Sinus-lifting," (in Japanese), *J. Robot. Soc. Jpn.*, vol. 26, no. 7, pp. 801-811, 2008
- [13] D. F. Hoyt and C. R. Taylor, "Gait and the energetics of locomotion in horses", *Nature*, Vol.292, no.16, pp.239-240, 1981.
- [14] F. Matsuno and H. Sato, "Trajectory tracking control of snake robot based on dynamic model," *Proc. IEEE Int. Conf. on Robotics and Automation*, pp. 3040-3046, 2005.
- [15] M. Tanaka and F. Matsuno, "A Study on Sinus-lifting Motion of a Snake Robot with Switching Constraints" *Proc. IEEE Int. Conf. on Robotics and Automation*, pp. 2270-2275, 2009
- [16] S. Toyoshima and F. Matsuno, "A Study on Sinus-lifting Motion of a Snake Robot with Energetic Efficiency" *Proc. IEEE Int. Conf. on Robotics and Automation*, pp. 2673-2678, 2012
- [17] F. Matsuno and K. Mogi, "Redundancy Controllable System and Control of Snake Robot with Redundancy based on Kinematic Model", *Proc. IEEE Conf. on Decision and Control*, pp. 4791-4796, 2000.
- [18] J. Nishii, "Legged insects select the optimal locomotor pattern based on the energetic cost," *Biological Cybernetics*, pp.435-442, 2000.